coatings

MDPI

Article

Surfaces Bearing Fluorinated Nucleoperfluorolipids for Potential Anti-Graffiti Surface Properties

Guilhem Godeau *, Frédéric Guittard and Thierry Darmanin *

NICE Lab, Université Côte d'Azur, IMREDD, Parc Valrose, 06100 Nice, France; guittard@unice.fr

* Correspondence: guilhem.godeau@unice.fr (G.G.); thierry.darmanin@unice.fr (T.D.)

Academic Editor: Mariateresa Lettieri

Received: 9 October 2017; Accepted: 24 November 2017; Published: 4 December 2017

Abstract: Graffiti can sometimes be a problem when put in an inappropriate place. We looked at a means to prevent such inconvenience. In this work, we explore the possibility of developing surfaces with controlled wettability. If the paint does not spread, the graffiti does not stay. Here, the synthesis and electrodeposition of original 3,4-ethylenedioxythiophene (EDOT) with perfluorinated nucleolipids (ante approach) is reported. The elaboration of similar surfaces using post functionalization is also described. All the prepared surfaces were then investigated for their roughness, wettability, and morphology. Highly hydrophobic features are reported ($\theta = 137°$) and oleophobic properties are also reported ($\theta = 110°$) showing real potential for the control of surface wettability and for potential anti-graffiti applications, consequently. The surfaces obtained with the ante approach are rougher and more hydrophobic.

Keywords: wettability; surface; electrodeposition; click chemistry; functionalization

1. Introduction

Surface wettability is a key parameter for a wide range of applications [1–4]. Among these applications, antigravity is one of particular interest [5,6]. The control of the paint spreading on surfaces is a powerful strategy to avoid monument degradation by unauthorized artwork. The control of the wettability is now well known and various examples have been observed in nature [7–10]. If the lotus leaf remains one of the more popular example, several other examples exist such as the rice leaf, the Echeveria leaf, water striders, fishing spiders, etc. Spectacular oleophobic properties have also been reported on springtails [11,12].

To explain these features, various models have been reported. One of the first described models is the Young–Dupré equation [13,14]. This equation is used to describe smooth surfaces and describe the apparent contact angle of a smooth surface (θ^Y) as a function of the interfacial tensions between three phases (liquid, solid, and gas). In the case of rough surfaces, two other equations that take into account the surface roughness exist [15,16]. One of these equations, the Wenzel equation [15], considers that the liquid deposed on a rough surface will enter all the surface roughness. The consequence of this equation is that it is possible to obtain high contact angle but only if $\theta^Y > 90°$. Moreover, high liquid adhesions between the liquid and the surface are often observed. The second equation is the Cassie–Baxter equation [16]. In this second model, the liquid stays on the top of the cavities, trapping some gas. In this case, it is possible to reach high contact angle whatever θ^Y. Moreover, the liquid adhesion can be ultra-low if the amount of air trapped inside the surface roughness is very important. Globally, these models enable the understanding that two parameters are of particular interest to control the surface wettability: surface energy and surface roughness [17,18]. Observations performed on springtails have also shown that, in the case of oleophobic features, a third parameter has to be considered [11,12]. The surface morphology should include reentrant cavities. The role of

these reentrant structures is to make negative Laplace pressure that prevent the oil from spreading. The elaboration of reentrant structures is a considerable challenge, a smart alternative is the use of perfluorinated chains. It is well established that due to their exceptional properties, perfluorinated chains lead to highly oleophobic properties. Indeed, due to specific properties of fluorine atoms—such as their high electronegativity and their higher atomic radius compared to hydrogen—fluorinated chains, and perfluorinated chains especially, are used to induce a high increase in both the surface hydrophobicity and oleophobicity.

To control all these parameters, various strategies have been used in the literature. Most of these approaches can be reported as top-down and bottom-up. The top down approach starts with smooth intrinsically hydrophobic material; this material is then structured with a treatment (such as plasma etching or acid engraving) [19]. The bottom-up approach starts with small hydrophobic building blocks or molecules [20]. These blocks are then self-assembled or polymerized. In this work, we focus on a particular bottom-up approach: the conductive polymer electrodeposition [21]. This approach has been reported as an efficient and unexpensive way to prepare highly hydrophobic surfaces in one step. The surface morphologies can be controlled by playing on the monomer chemistry and the electrodeposition conditions while the surface energy can be controlled by grafting a hydrophobic substituent. Here, the selected monomers are made of 3,4-ethylenedioxythiophene (EDOT) derivatives [22]. The EDOT has been selected due to their exceptional properties for polymerization. A nucleoside part was grafted to initiate self-organization during the polymerization [23,24]. To lead to intrinsic hydrophobic and oleophobic properties, perfluorinated chains were also added to the monomer. The grafting of the perfluorinated chains was achieved using the Staudinger–Vilarrasa reaction [25]. The Staudinger–Vilarrasa reaction is known as a click-like reaction. This reaction has been successfully used to functionalize monomers before polymerization (ante approach) or to functionalize the surface after polymerization (post approach) [26].

In this work, we report for the first time the use of the Staudinger–Vilarrasa reaction to prepare hydrophobic/oleophobic surfaces based on perfluoronucleolipid (Figure 1). The developed monomers were polymerized and the surfaces were then studied for their roughness, morphology, and wettability. Surface properties developed using ante and post approaches are also compared.

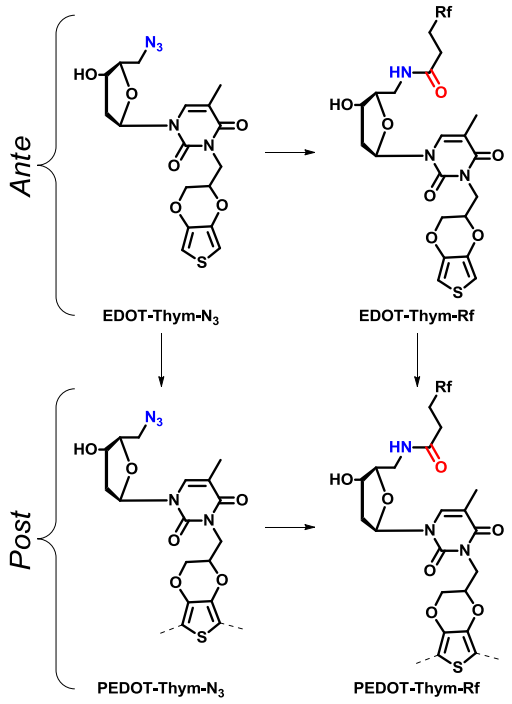

Figure 1. General procedure for surface elaboration.

2. Materials and Methods

2.1. Synthesis

Synthesis of (4-bromobutyl)-ethylenedioxythiophene (EDOT-Br) and 5′-azidothymidine (Scheme 1) has been schieved following the procedure described in the literature. All spectroscopic data match with the one described in the literature [22,27].

Synthesis of EDOT-Thym-N_3: 5′-N_3-thymidine (482 mg, 1.8 mmol, 1 eq) and EDOT-Br (500 mg, 1.8 mmol) were dissolved in DMF. Potassium carbonate (685 mg, 3.6 mmol, 2 eq) was added. The mixture was stirred at 90 °C overnight. The mixture was then allowed to cool down at room temperature (Scheme 2). The DMF was removed under reduced pressure EDOT-Thym-N_3 is finally purified on column (50/50, cyclohexane/ethyl acetate).

Yield: 66%; Colorless oil; δ_H(200 MHz, $CDCl_3$, ppm): 7.4 (s, 1H), 6.3 (s, 2H), 6.1–6.2 (m, 1H), 3.6–4.2 (m, 8H), 2.6–2.8 (m, 1H), 2.1–2.2 (m, 2H), 1.9 (s, 3H), 1.56–1.66 (m, 8H); δ_C (50 MHz, $CDCl_3$, ppm): 163.1, 150.1, 142.1, 141.6, 133.0, 110.5, 99.3, 99.2, 84.4, 80.3, 73.5, 68.4, 50.0, 41.0, 38.4, 30.2, 27.3, 22.4, 13.5.

Synthesis of EDOT-Thym-F_n: Perfluorinated acid (0.48 mmol), DMAP (88 mg, 0.72 mmol) and EDCI (111 mg, 0.58 mmol) were dissolved in THF. The mixture was stirred for 30 min. Tributylphosphine was added (242 µL, 0.96 mmol) and after EDOT-Thym-N_3 (150 mg, 0.32 mmol). The mixture was stirred for 3 h at room temperature. The solvent was then removed under reduced pressure. The EDOT-Thym-F_n were finally purified on column (100/0 to 50/50, cyclohexane/ethyl acetate).

- Synthesis of EDOT-Thym-F_4

Yield: 36%; Colorless oil ; δ_H(200 MHz, $CDCl_3$, ppm): 8.2 (m, 1H), 7.0 (m, 1H), 6.2 (s, 2H), 6.1–6.2 (m, 1H), 3.6–4.2 (m, 8H), 2.4–2.7 (m, 2H), 1.9–2.0 (m, 4H), 1.9 (s, 3H), 1.56–1.66 (m, 8H); δ_C (50 MHz, $CDCl_3$, ppm): 169.9, 169.4, 162.0, 149.7, 141.0, 140.6, 138.3, 113.0, 110.0, 98.4, 98.3, 90.7, 72.5, 67.3, 48.9, 40.0, 30.9, 29.3, 28.5; 26.2, 21.7, 13.1; δ_F(188 MHz, $CDCl_3$, ppm): −81.1, −115.0, −124.6, −126.2.

- Synthesis of EDOT-Thym-F_6

Yield: 47%; Colorless oil; δ_H(200 MHz, $CDCl_3$, ppm): 8.2 (m, 1H), 6.9 (m, 1H), 6.2 (s, 2H), 5.7–5.8 (m, 1H), 3.6–4.2 (m, 8H), 2.4–2.7 (m, 2H), 1.9–2.0 (m, 4H), 1.9 (s, 3H), 1.56–1.66 (m, 8H); δ_C (50 MHz, $CDCl_3$, ppm): 170.0, 169.3, 162.0, 149.7, 141.0, 140.6, 138.3, 113.0, 110.0, 98.3, 98.3, 90.8, 72.5, 67.3, 48.9, 40.0, 30.9, 29.2, 28.5; 26.2, 21.7, 13.1; δ_F(188 MHz, $CDCl_3$, ppm): −80.9, −114.8, 122.1, 123.1, −123.7, −126.3.

- Synthesis of EDOT-Thym-F_8

Yield: 52%; Colorless oil; δ_H(200 MHz, $CDCl_3$, ppm): 8.2 (m, 1H), 6.9 (m, 1H), 6.3 (s, 2H), 6.1–6.2 (m, 1H), 3.6–4.2 (m, 8H), 2.4–2.7 (m, 2H), 1.9–2.0 (m, 4H), 1.9 (s, 3H), 1.56–1.66 (m, 8H); δ_C (50 MHz, $CDCl_3$, ppm): 170.0, 169.3, 162.0, 149.7, 141.0, 140.6, 138.3, 113.0, 110.0, 98.3, 98.3, 90.8, 72.5, 67.3, 48.9, 40.0, 30.9, 29.2, 28.5; 26.2, 21.7, 13.1; δ_F(188 MHz, $CDCl_3$, ppm): −80.8, −114.8, −122.1, −122.8, −123.7, −126.3.

2.2. General Procedure for Electropolymerization

In a glass cell containing a solution of tetrabutylammonium perchlorate (0.1 M) in anhydrous acetonitrile, the monomer was inserted (0.01 M). Three electrodes were put inside the solution. A 2 cm^2 gold plate (purchased from Neyco, Vanves, France) (working electrode), glassy carbon rods (counter electrode), and saturated calomel electrodes (SCE) (reference electrode) were used. The three electrodes were connected to an Autolab potentiostat (Metrohm, Herisau, Switzerland). Before each experiment, the solution was degassed under argon. After the deposition, the samples were cleaned in three different acetonitrile solutions to remove the remaining salts.

2.3. General Procedure for PEDOT Surface Modification

In a 25 mL reactor, 100 mg of perfluorinated acid were dissolved in 5 mL of THF (anhydrous). 100 mg (0.82 mmol) of *N*,*N*-dimethylaminopyridine and 100 mg (0.64 mmol) of 1-ethyl-3-(3-dimethylaminopropyl)carbodiimide were added. The mixture was shaken for 30 min. The PEDOT-Thym-N_3 (3 scans) substrate was introduced and then 100 mg (0.49 mmol) of tributylphosphine. The mixture was shaken for 3 h. The substrate was then washed three times with water and three times with ethanol and dried.

2.4. Surface Characterization

The apparent and dynamic contact angles were obtained with a DSA30 goniometer of Krüss (Hamburg, Germany). Apparent contact angles were measured using the sessile drop method and the dynamic one was obtained with the tilted drop method. In this last method, a surface, on which a 2 µL water droplet was placed, is inclined until the droplet rolls off. If the water drop did not slide for angles higher than 90°, the surface is described as sticky or parahydrophobic. The mean arithmetic (R_a) roughness were measured by optical profilometry using Wyko NT 1100 from Bruker (Billerica, MA, USA). The measurements were realized with high mag phase shift interference (PSI), objective ×50, and field of view ×0.5. All experiments were performed three times to get the standard deviation. Scanning electron microscopy was performed using a JEOL 6700F (Tokyo, Japan).

3. Results

3.1. Synthesis

In this work, the used monomer is an important parameter. Here, we decided to use nucleoside hybrid monomer as base for surface elaboration. To reach this goal, a nucleoside part is linked to a monomer suitable for electrodeposition. Here the used monomer is derived from the 3,4-ethylenedioxythiophene (EDOT) due to its exceptional electronic properties. Due to the particularly simple handling of the thymidine, this nucleoside has been selected. Also, the thymidine building block is known to accept multiple modifications both on the pyrimidine part or on the sugar. Of course, the functionalization on the pyrimidine part will avoid a possible nucleic interaction with other nucleosides like adenosine. However, this modification will not decrease the potential self-assembly as reported in the literature for perfluorinated glyconucleolipids. Following a similar approach to glyconucleolipid elaboration, the first step here was the elaboration of thymidine monomer suitable for both final functionalization and grafting on monomer. The grafting was made using N-alkylation on the thymine part. To allow the final functionalization, an azido group was grafted on the 5′ position of the sugar. The 5′-azido-5′-deoxythymidine was prepared in two steps following a procedure reported in the literature (Scheme 1).

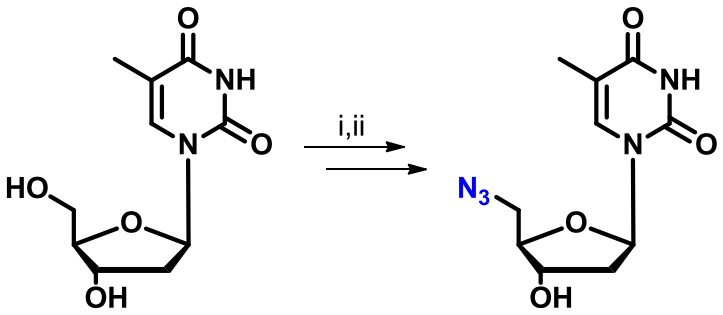

Scheme 1. Synthesis of 5′-azidothymidine. (**i**) Methanesulfonyl chloride (2 eq), triethylamine (3 eq), dichloromethane, rt, 4 h; (**ii**) Sodium azide (5 eq), DMF, 95 °C, overnight.

The first part is the preparation of the corresponding 5′-methanesulfonyl ester on the thymidine. This reaction was carried out in DCM with triethylamine and methanesulfonyl chloride at room temperature over 3 h. The formed sulfonyl ester was directly used for the next step without further purification. The crude mixture was dissolved in DMF and sodium azide was added. The mixture was then reacted overnight at 95° and the aimed N_3-thymidine was obtained.

Next, EDOT derivate suitable for N-alkylation was prepared (Scheme 2).

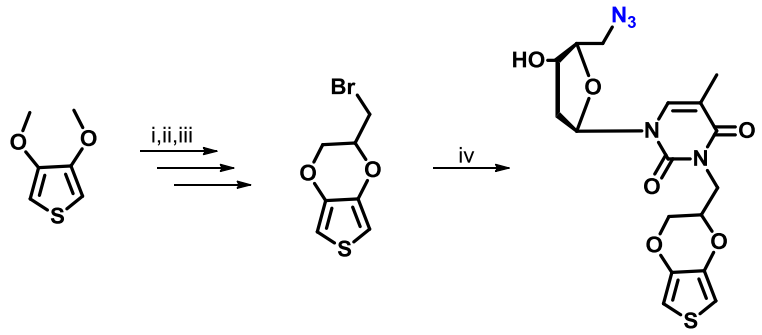

Scheme 2. Synthesis of EDOT-Thym-N_3: (**i**) Hexan-1,2,6-triol (2 eq), *para*-toluenesulfonic acid (0.01 eq), toluene reflux, 36 h; (**ii**) Methanesulfonyl chloride (1.2 eq), triethylamine (2 eq), dichloromethane, rt, 4 h; (**iii**) potassium bromide (5 eq), DMF, 95 °C, overnight; (**iv**) 5′-azidothymidine (1 eq), K_2CO_3 (2 eq), DMF, 90 °C, overnight.

This 4-bromobutyl-EDOT has been prepared in three steps following the procedure described in the literature. Shortly, the synthesis can be described as a sequence of transetherification, sulfonyl ester formation and nucleophilic substitution. The transetherification between 3,4-dimethoxythiophene and hexan-1,2,6-triol was carried out in toluene at 95° with para-toluenesulfonic acid as catalyst. The reaction ran over 36 h. The corresponding methansulfonyl ester was prepared following a procedure similar compared to the one described for the thymidine. The final nucleophilic substitution was performed in DMF with potassium bromide at 95 °C overnight. Finally, the EDOT part and the thymidine were linked together using N-alkylation with potassium carbonate in DMF at room temperature to form the EDOT-Thym-N_3.

The formed EDOT-Thym-N_3 was suitable for functionalization using the Staudinger–Vilarrasa reaction (Scheme 3).

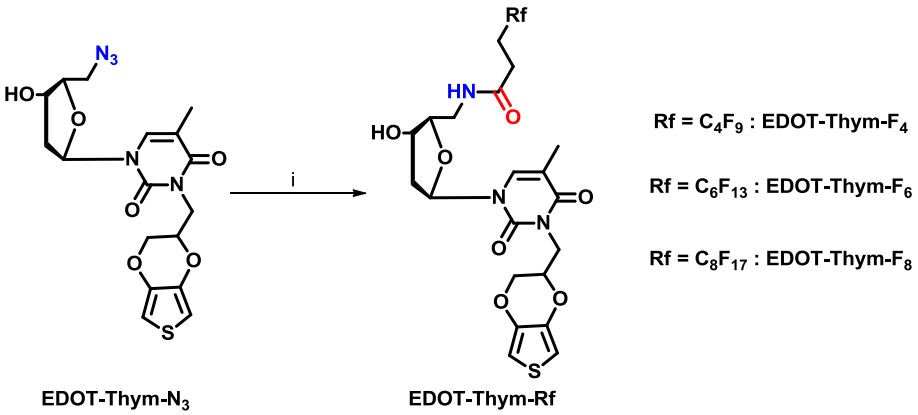

Scheme 3. Synthesis of EDIT-Thym-Rf. (**i**) perfluorinated carboxylic acid, 1-ethyl-3-(3-dimethylaminopropyl)carbodiimide, *N*,*N*-dimethylaminopyridine, tributylphosphine, THF, rt, 3 h.

This reaction was performed in THF. First, tributylphosphine was added to form the corresponding reactive iminophosphorane that react with activated perfluorinated carboxylic acid

to form the corresponding amide. In this work, three perfluorinated chain length were studied. The carboxylic acids were activated using conventional EDCI, DMAP strategy. The iminophosphorane was initially formed over 30 min before addition of the activated carboxylic acid. The final amidification ran over 3 h.

3.2. Electrodeposition

All the prepared monomers were suitable for electrodeposition and were electropolymerized on gold covered wafers as working electrode using a cyclic voltammetry procedure. The electropolymerization was carried out in tetrabutylammonium perchlorate (Bu_4NClO_4) acetonitrile solution. All the monomer oxidation potentials were measured vs. saturated calomel electrode (SCE) and the polymers were deposed from −1 V to a potential close from the monomer oxidation potential with a scan rate of 20 mV/s. All the oxidation potential and polymerization range are reported Table 1.

Table 1. Electrochemical data.

Momomer	Oxydation Potention (V)	Depostion Range (V)
EDOT-T-N3	1.49	−1 to 1.45
EDOT-T-F4	1.44	−1 to 1.38
EDOT-T-F6	1.48	−1 to 1.46
EDOT-T-F8	1.47	−1 to 1.43

In order to consider the influence of the polymer growth on surface properties different number of deposition scans were performed (1, 3, and 5). The cyclic voltammograms after five deposition scans are given in Figure 2.

As shown on the voltammograms, both compounds polymerized correctly and gave relatively well-defined cyclic voltammograms. Steric hindrance was observed during polymerization, which was expected due to the large size of the substituent.

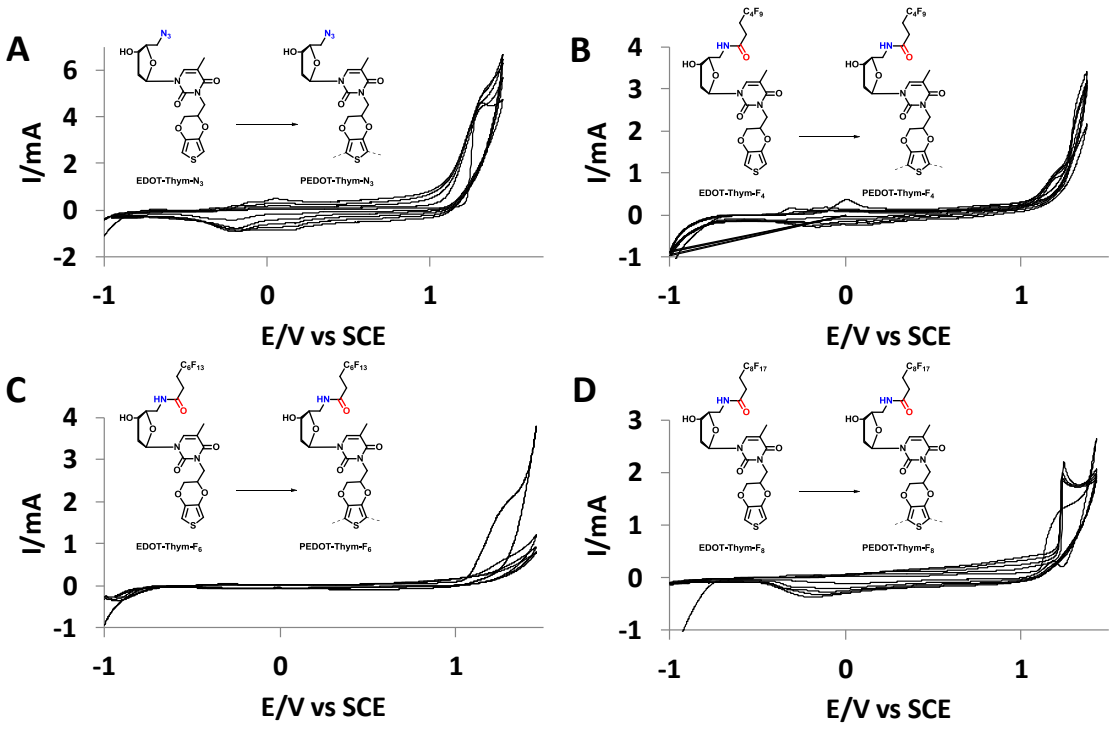

Figure 2. Examples of voltammogram. (**A**) EDOT-Thym-N_3 to PEDOT-Thym-N_3; (**B**) EDOT-Thym-F_4 to PEDOT-Thym-F_4; (**C**) EDOT-Thym-F_6 to PEDOT-Thym-F_6; (**D**) EDOT-Thym-F_8 to PEDOT-Thym-F_8.

3.3. PEDOT-Thym-N_3 Post-Functionalization

As reported for PEDOT-N_3 surfaces, the possibility of the surface post-functionalizations were investigated (Figure 3).

To post-functionalize the surfaces, only the three scan surfaces were chosen. The post-functionalization was carried out in THF. First, tributylphosphine was reacted on PEDOT-Thym-N_3 substrates to form the corresponding iminophosphorane surfaces. These surfaces were then reacted with an activated perfluorinated carboxylic acid to reach the corresponding PEDOT-T-F_n (n = 4, 6 or 8) surfaces.

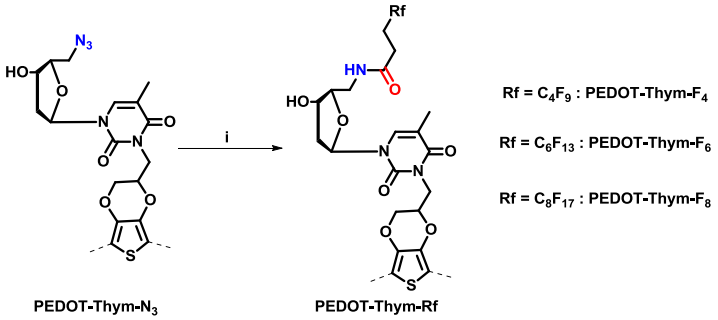

Figure 3. Global procedure for post-functionalization. (**i**) perfluorinated carboxylic acid, 1-ethyl-3-(3-dimethylaminopropyl)carbodiimide, *N*,*N*-dimethylaminopyridine, tributylphosphine, THF, rt, 3 h.

3.4. Surface Roughness

After their deposition, all surfaces were investigated for their roughness (Figure 4).

For the surfaces developed using the ante strategy, it is possible to observe that the surface roughness increases depending on both the perfluorinated chain length and the number of deposition scans. Only PEDOT-T-F_6 shows a significant decrease of the roughness after five scans. For the post-functionalized surfaces, it is possible to note that the post-functionalization did not change the surface roughness. This result is consistent with observation reported on the literature about surface post-functionalization with the Staudinger–Vilarrasa reaction.

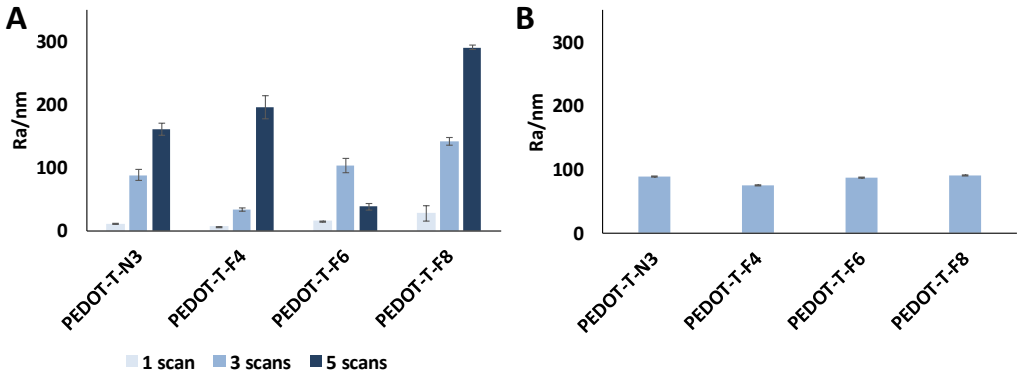

Figure 4. Roughness measurement for surfaces elaborated with ante strategy (**A**) and post strategy (**B**). The bars on the columns illustrate the standard deviations of the measurements.

3.5. Surface Wettability

All the developed surfaces were then investigated for their wettability. Two different probe liquids were considered: water and diiodomethane and all measured angles are presented Table 2.

The results observed for surfaces prepared using both the ante and post strategies are reported Figure 5A,B, respectively.

Table 2. Apparent contact angles with water and diiodomethane (all values are reported in degree).

Water		**PEDOT-T-N_3 (°)**	**PEDOT-T-F_4 (°)**	**PEDOT-T-F_6 (°)**	**PEDOT-T-F_8 (°)**
Ante	1 scan	73 ± 0.5	103 ±1	118 ± 1	115 ± 3
	3 scans	72 ± 2	113 ± 1	131 ± 1	125 ± 1
	5 scans	77 ± 2	123 ± 1.5	117 ± 1	137 ± 1
Post	3 scans	72 ± 2	106.5 ± 2	117 ± 1	112 ± 3
CH_2I_2		–	**PEDOT-T-F_4 (°)**	**PEDOT-T-F_6 (°)**	**PEDOT-T-F_8 (°)**
Ante	1 scan	–	81 ± 4	98 ± 2	95 ± 4
	3 scans	–	92 ± 2	110 ± 1	102 ± 3
	5 scans	–	104 ± 2	91 ± 6	118 ± 1
Post	3 scans	–	84 ± 5	97 ± 3	83 ± 4

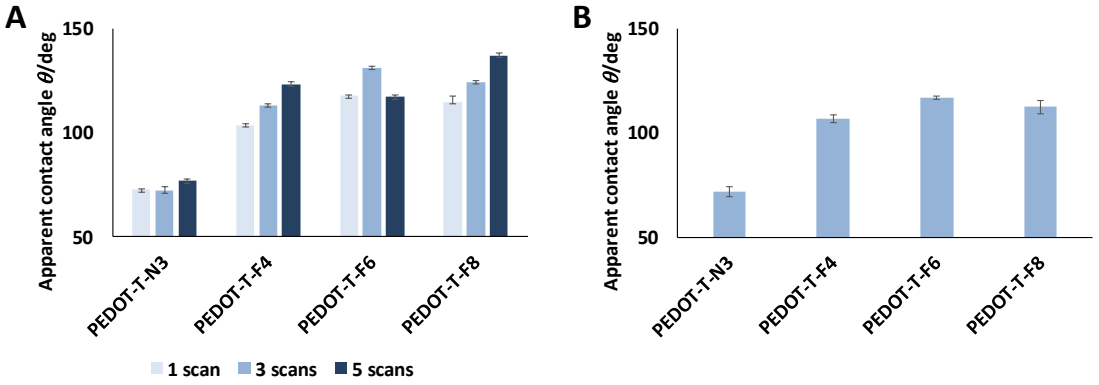

Figure 5. Apparent contact angle with water measured for surfaces developed with ante strategy (**A**) and post strategy (**B**). The bars on the columns illustrate the standard deviations of the measurements.

As expected, it is possible to note that the surfaces bearing perfluorinated chains present higher contact angles compared to the surfaces with the azido group. This change is due to the chemical change of the surface and as consequence the surface energy. Not surprisingly, the surface without prefluorinated chains can be reported as hydrophilic whatever the number of deposition scans θ = 73°, θ = 72°, and θ = 77° for PEDOT-Thym-N_3 after 1, 3, and 5 scans. In the case of perfluorinated surfaces developed using the ante strategy, it is possible to observe that in most of the case the hydrophobic properties increase with the increase of the deposition scan number. This result is consistent with the increase of the surface roughness due to the accumulation of polymer. Only the θ value observed for the five surface PEDOT-T-F_6 scans presents a decrease in hydrophobic feature compared to the three scans value. This result is consistent with the decrease in roughness observed for PEDOT-T-F_6 after five scans. Interestingly, even if the surfaces bear perfluorinated chains, none of these surfaces can be reported as superhydrophobic. The higher contact angle observed was θ = 137° and has been observed for five PEDOT-T-F_8 scans. Interestingly, even the more hydrophobic surfaces remain adherent with water. A water drop deposed on the surface remain stuck even if the surface is tilted with angle of 90°. All surfaces can be reported as parahydrophobic [18].

For post-functionalized surfaces, it is interesting to note that all surfaces present slightly hydrophobic properties after the post-functionalization with θ = 106°, θ = 117°, and θ = 112° for PEDOT-T-F_4, PEDOT-T-F_6, and PEDOT-T-F_8 respectively. This increase in hydrophobic feature is fully consistent with the grafting of the perfluorinated chains that decrease the surface energy.

To complete the wettability study, the measurements were performed with diiodomethane as a probe liquid (Figure 6).

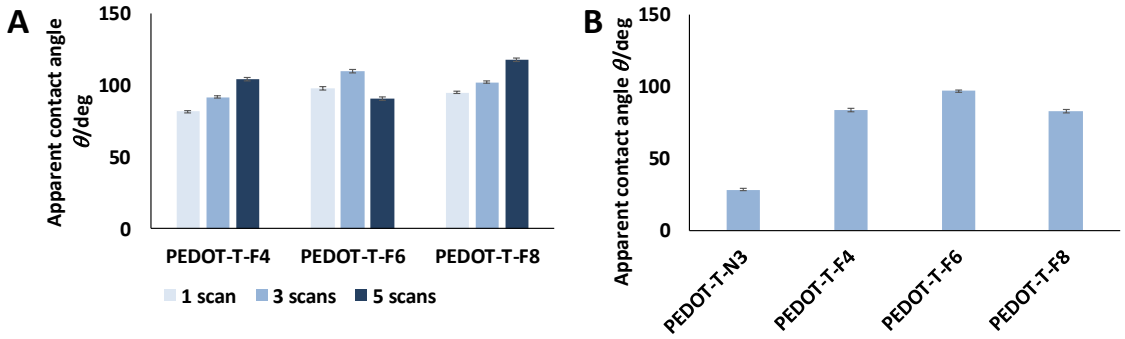

Figure 6. Apparent contact angle with diiodomethane measured for surfaces developed with ante strategy (**A**) and post strategy (**B**). The bars on the columns illustrate the standard deviations of the measurements.

For the ante functionalized surfaces, the apparent contact angle increases depending on the perfluorinated chain length and the number of deposition scans. This result is very interesting and confirms the importance of both surface energy (perfluorinated chain length) and morphology (number of scan). Except for PEDOT-T-F_6 after five scans as for the results observed with water. As for the results observed with water, all the results observed on post functionalized surfaces with diiodomethane present similar apparent contact angles near 110°. Unfortunately, all the surfaces appear clearly oleophilic with hexadecane.

3.6. Surface Morphology

To completely explain the wettability results, the surface morphologies were investigated with SEM. The morphologies observed for ante functionalized surfaces are reported in Figure 7.

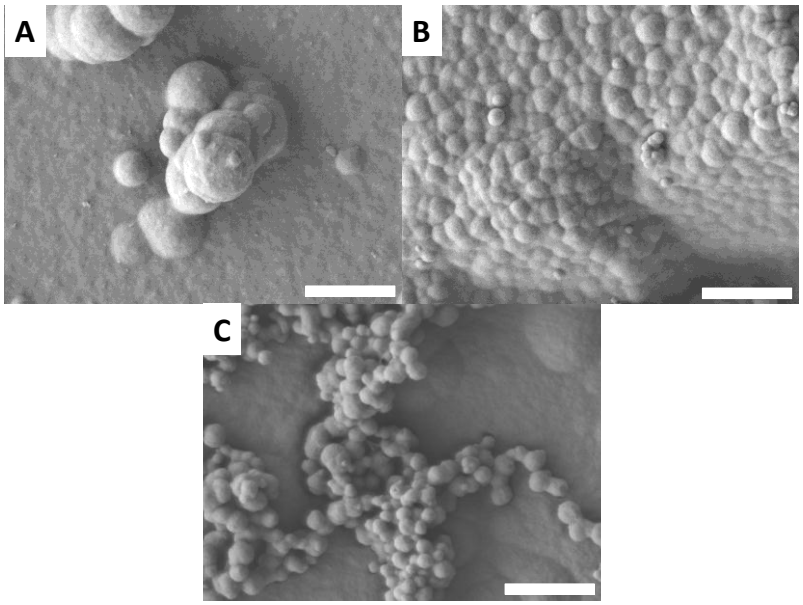

Figure 7. Morphologies observed for surfaces developed using *ante* strategy (scale bar = 1 µm). (**A**) PEDOT-Thym-F_4 three scans; (**B**) PEDOT-Thym-F_6 three scans; (**C**) PEDOT-Thym-F_8 three scans.

Interestingly, all surfaces present assembly of spherical particles. Such structures are regularly described in the literature for perfluorinated surfaces developed using electrodeposition. In this case, we can observe that morphology seems to be led by the perfluorinated part without significant impact of the nucleoside part. As confirmation of the roughness measurements, the SEM images show an increase of the surface structuration according with the increase of the perfluorinated chain length.

SEM images on post-functionalized surfaces also confirm roughness observation (Figure 8). The surfaces are relatively smooth.

The surface morphology remains similar for PEDOT-Thym-N_3 and for post-functionalized surfaces. As mentioned in the roughness part, these results are highly relevant compared with the literature. In both ante and post functionalized surfaces, no reentrant cavities were observed. This observation can explain the low oleophobic feature observed for the perfluorinated surfaces.

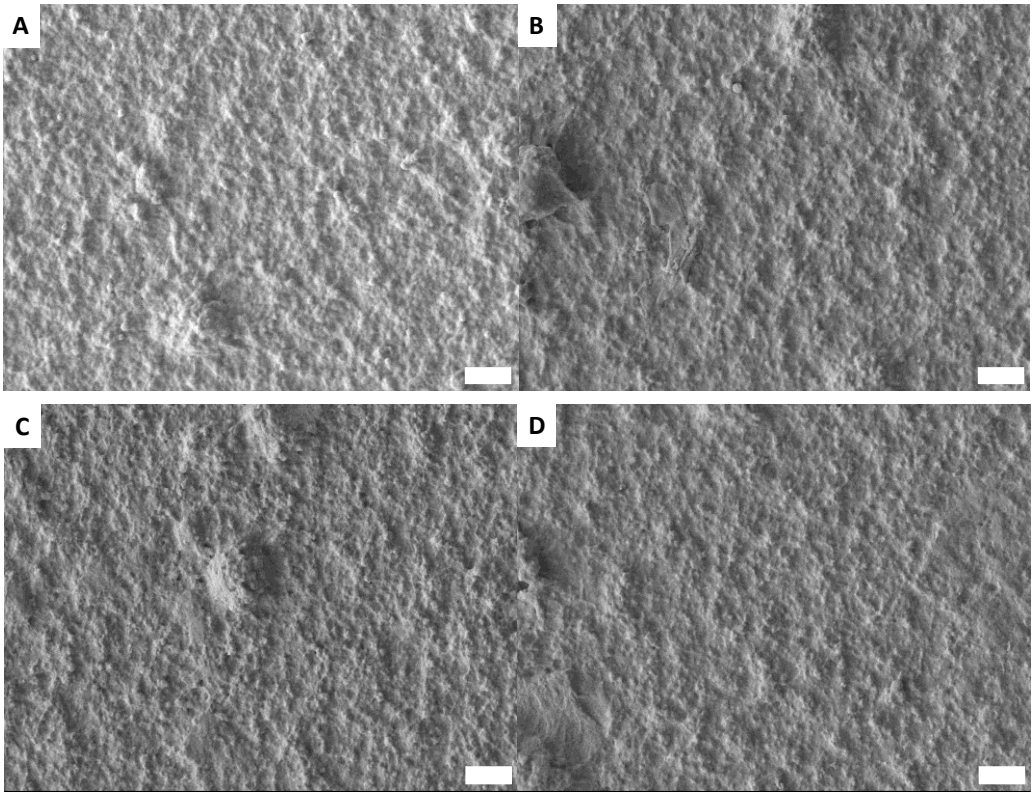

Figure 8. Morphologies observed for surfaces developed using post strategy (scale bar = 1 μm). (**A**) PEDOT-Thym-N_3; (**B**) PEDOT-Thym-F_4; (**C**) PEDOT-Thym-F_6; (**D**) PEDOT-Thym-F_8.

4. Conclusions

In this work, we reported for the first time preparation—using both ante and post functionalization—of PEDOT surfaces with perfluorinated nucleolipids. The surface developed using the post strategy gave similar results for all the used perfluorinated chains. Interestingly, only the surfaces developed using ante strategy present different results depending on the perfluorinated chain length and the number of deposition scans. The surfaces were prepared using the Staudinger Vilarrasa reaction. All the perfluorinated surfaces were highly hydrophobic and showed low oleophobic features but the surfaces obtained with the ante approach were rougher and more hydrophobic compared to the surfaces prepared by post-functionalization. If the initial results to be directly used as an anti-graffiti strategy, the observed results are encouraging and the electrodeposition of monomers with perfluorinated nucleolipid seems to be a promising strategy for future work.

Acknowledgments: We thank François Orange of the Centre Commun de Microscopie Appliquée (CCMA, Université Nice Sophia Antipolis) for the SEM Images.

Author Contributions: Guilhem Godeau and Thierry Darmanin conceived and designed the experiments; Guilhem Godeau performed the experiments; Guilhem Godeau and Thierry Darmanin analyzed the data; Frédéric Guittard contributed reagents/materials/analysis tools. All three authors wrote the paper.

Conflicts of Interest: The authors declare no conflicts of interest.

References

1. Darmanin, T.; Guittard, F. Recent advances in the potential applications of bioinspired superhydrophobic materials. *J. Mater. Chem. A* **2014**, *2*, 16319–16359. [CrossRef]
2. Su, B.; Tian, Y.; Jiang, L. Bioinspired interfaces with superwettability: From materials to chemistry. *J. Am. Chem. Soc.* **2016**, *138*, 1727–1748. [CrossRef] [PubMed]
3. Liu, M.; Zheng, Y.; Zhai, J.; Jiang, L. Bioinspired super-antiwetting interfaces with special liquid–Solid adhesion. *Acc. Chem. Res.* **2010**, *43*, 368–377. [CrossRef] [PubMed]
4. Yu, S.; Guo, Z.; Liu, W. Biomimetic transparent and superhydrophobic coatings: From nature and beyond nature. *Chem. Commun.* **2015**, *51*, 1775–1794. [CrossRef] [PubMed]
5. Rabea, A.M.; Mohseni, M.; Mirabedini, S.M.; Tabatabaei, M.H. Surface analysis and anti-graffiti behavior of a weathered polyurethane-based coating embedded with hydrophobic nano silica. *Appl. Surf. Sci.* **2012**, *258*, 4391–4396. [CrossRef]
6. Lettieri, M.; Masieri, M. Surface characterization and effectiveness evaluation of anti-graffiti coatings on highly porous stone materials. *Appl. Surf. Sci.* **2014**, *288*, 466–477. [CrossRef]
7. Darmanin, T.; Guittard, F. Superhydrophobic and superoleophobic properties in nature. *Mater. Today* **2015**, *18*, 273–285. [CrossRef]
8. Koch, K.; Bhushan, B.; Barthlott, W. Multifunctional surface structures of plants: An inspiration for biomimetics. *Prog. Mater. Sci.* **2009**, *54*, 137–178. [CrossRef]
9. Sun, Z.; Liao, T.; Liu, K.; Jiang, L.; Kim, J.H.; Dou, S.X. Fly-eye inspired superhydrophobic anti-fogging inorganic nanostructures. *Small* **2014**, *10*, 3001–3006. [CrossRef] [PubMed]
10. Watson, G.S.; Green, D.W.; Schwarzkopf, L.; Li, X.; Cribb, B.W.; Myhra, S.; Watson, J.A. A gecko micro/nano structure—A low adhesion, superhydrophobic, anti-wetting, self-cleaning, biocompatible, antibacterial surface. *Acta Biomater.* **2015**, *21*, 109–122. [CrossRef] [PubMed]
11. Hensel, R.; Neinhuis, C.; Werner, C. The springtail cuticle as a blueprint for omniphobic surfaces. *Chem. Soc. Rev.* **2016**, *45*, 323–341. [CrossRef] [PubMed]
12. Hensel, R.; Neinhuis, C.; Werner, C. Wetting resistance at its topographical limit: The benefit of mushroom and serif T structures. *Langmuir* **2013**, *29*, 1100–1112. [CrossRef] [PubMed]
13. Young, T. An essay on the cohesion of fluids. *Philos. Trans. R. Soc. Lond.* **1805**, *95*, 65–87. [CrossRef]
14. Bormashenko, E. Physics of solid–liquid interfaces: From the Young equation to the superhydrophobicity. *Low Temp. Phys.* **2016**, *42*, 622–635. [CrossRef]
15. Wenzel, R.N. Resistance of solid surfaces to wetting by water. *Ind. Eng. Chem.* **1936**, *28*, 988–994. [CrossRef]
16. Cassie, A.B.D.; Baxter, S. Wettability of porous surfaces. *Trans. Faraday Soc.* **1944**, *40*, 546–551. [CrossRef]
17. Marmur, A. From hygrophilic to superhygrophobic: Theoretical conditions for making high-contact-angle surfaces from low-contact-angle materials. *Langmuir* **2008**, *24*, 7573–7579. [CrossRef] [PubMed]
18. Marmur, A. Wetting on hydrophobic rough surfaces: To be heterogeneous or not to be? *Langmuir* **2003**, *19*, 8343–8348. [CrossRef]
19. Zha, J.; Batisse, N.; Claves, D.; Dubois, M.; Frezet, L.; Kharitonov, A.P.; Alekseiko, L.N. Superhydrophocity via gas-phase monomers grafting onto carbon nanotubes. *Prog. Surf. Sci.* **2016**, *91*, 57–71. [CrossRef]
20. Chu, Z.; Olveira, S.; Seeger, S. A facile, sustainable strategy towards the preparation of silicone nanofilaments and their use as antiwetting coatings. *ChemistrySelect* **2017**, *2*, 5463–5468. [CrossRef]
21. Mortier, C.; Darmanin, T.; Guittard, F. Direct electrodeposition of superhydrophobic and highly oleophobic poly(3,4-ethylenedioxypyrrole (PEDOP) and poly(3,4-propylenedioxypyrrole) (PProDOP) nanofibers. *ChemNanoMat* **2017**. [CrossRef]
22. Godeau, G.; Darmanin, T.; Guittard, F. Nucleoside surface as platform for the control of surface hydrophobicity. *RSC Adv.* **2016**, *6*, 62471–62477. [CrossRef]

23. Godeau, G.; Barthélémy, P. Glycosyl-nucleoside lipids as low-molecular-weight gelators. *Langmuir* **2009**, *25*, 8447–8450. [CrossRef] [PubMed]
24. Dolain, C.; Patwa, A.; Godeau, G.; Barthélémy, P. Nucleic acid based fluorinated derivatives: New tools for biomedical applications. *Appl. Sci.* **2012**, *2*, 245–259. [CrossRef]
25. Burés, J.; Martín, M.; Urpí, F.; Vilarrasa, J. Catalytic Staudinger-Vilarrasa reaction for the direct ligation of carboxylic acids and azides. *J. Org. Chem.* **2009**, *74*, 2203–2206. [CrossRef] [PubMed]
26. Godeau, G.; Darmanin, T.; Guittard, F. Ante versus post-functionalization to control surface structures with superhydrophobic and superoleophobic properties. *RSC Adv.* **2015**, *5*, 63945–63951. [CrossRef]
27. Godeau, G.; Staedel, C.; Barthélémy, P. Lipid-conjugated oligonucleotides via "click chemistry" efficiently inhibit hepatitis C virus translation. *J. Med. Chem.* **2008**, *51*, 4374–4376. [CrossRef] [PubMed]